Crack initiation behavior of notched specimens on heat resistant steel under service type loading at high temperature

Lu Cui
School of mechanical Engineering, Xi'an Shiyou UniversityUniversity
Institut für Werkstoffkunde, Technische Universität Darmstadt
cuiluxa@hotmail.com

Peng Wang
BorgWarner Turbo Systems Engineering GmbH
Institut für Werkstoffkunde, Technische Universität Darmstadt
Wp168@hotmail.com

ABSTRACT. Cracks at notches deserve special consideration in the design of steam turbine components. This work is addressed to investigate the crack initiation behavior a 10%Cr rotor steel with the help of notched specimens under service-type loading. A significant drifting down of the peak-values of axial deformation under constant amplitude load was observed. Crack initiation was evaluated with the help of the relationship between irreversible deformation energy and cycle number. Further, metallographic examinations were employed to characterize the superposition of creep and fatigue damage mechanisms. Both Neuber-hypothesis and von Mises equivalent strain at notch root were applied for lifetime prediction. Finally, the effectiveness of both methods is validated by comparing with experimental results.

KEYWORDS. 10%Cr steel; Notched; Lifetime; Neuber; von Mises.

OPEN ACCESS

Citation: Cui, L., Wang, P., Crack initiation behavior of notched specimens on heat resistant steel under service type loading at high temperature, Frattura ed Integrità Strutturale, 38 (2016) 26-35.

Received: 14.05.2016
Accepted: 20.06.2016
Published: 01.10.2016

INTRODUCTION

Steam turbine components are subjected to quasi-static primary loading due to steam pressure superimposed by variable secondary loading due to temperature transients in start-up and shut-down processes. The difference between the surface temperature and the average core temperature leads to compression strains during start-up and tension strains during shut-down (Fig. 1). At stationary service, the turbine temperature reaches quasi-balance, and the compression and tension stresses relax during the hold time. Due to stress concentration, notches lead to a further decrease of lifetime [1].

In previous studies, notch behavior on rotor steel of X12CrMoWVNbN10-1-1 was investigated by conventional low cycle fatigue tests without dwell time (LCF-cycles) and creep fatigue tests with hold times at maximum and minimum load on notched specimens [2]. However the knowledge gained from those experiments are still insufficient to exploit the full potential of this steel. This requires experiments on notched specimen to understand the practical implications of applying such an approach to a service situation.

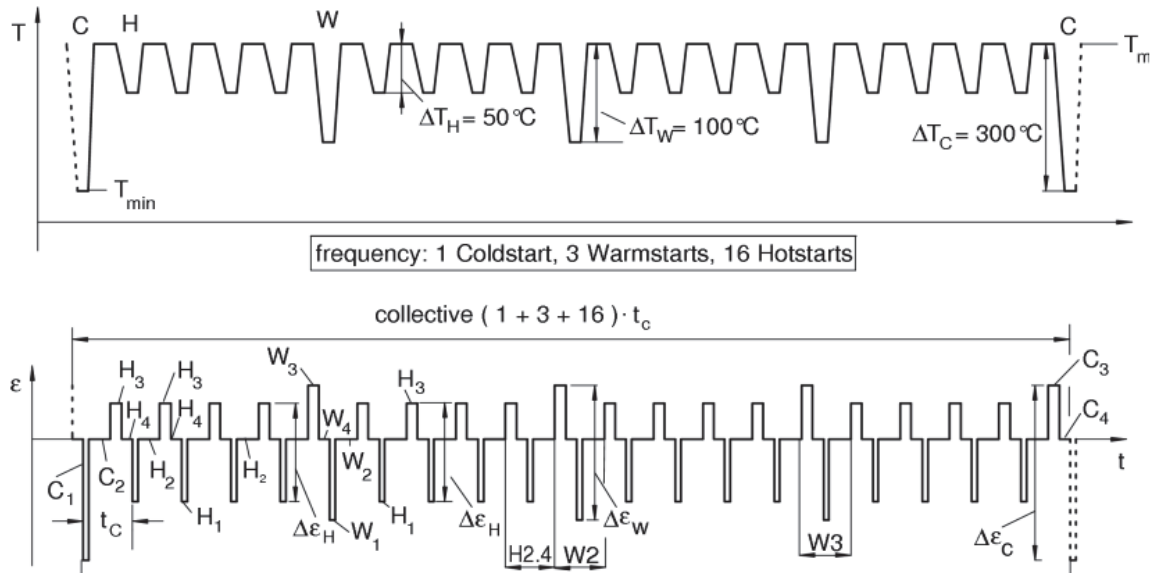

Figure 1: Three stage service-type strains cycling at heated surface of power plant components

A phenomenological lifetime estimation method which was developed for a multistage service-type creep fatigue loading, specially demonstrates the applicability of rules for synthesis of stress strain path and relaxation including an internal stress concept, as well as mean stress effects. Further, a modified linear damage rule for creep-fatigue life estimation was employed, and a creep fatigue interaction concept covering a wide range of creep dominant loading as well as fatigue dominant loading was also developed. To describe multiaxial stress state at notch, the Neuber hypothesis was applied. In addition, the service-type loading was also analyzed with finite-element-calculation and an equivalent loading is determined. In the end, the lifetime estimation model was validated with the experiments performed in this study.

EXPERIMENTAL

Material

The tested material is a modern ferritic-martensitic stainless steel of type 10Cr-1Mo-1W-V-Nb (German grade X12CrMoWVNbN10-1-1), which is proposed to be suitable for high temperature applications up to 600°C/300bar. Chemical composition and heat treatment of the material are introduced in [3] and listed in Tab. 1. Test specimens were manufactured from the same heat. Because the maximal thermal damage occurs on the heated surface of a rotor, the specimens were taken from locations close to the periphery of production forging with a longitudinal orientation with respect to the axis of the rotor.

	C	Cr	Mo	W	Ni	V	Nb	N	Mn	Si	P
X12CrMoWVNbN10-1-1	0.12	10.7	1.04	1.04	0.76	0.16	0.05	0.06	0.42	0.1	0.007
manufacturing	segment of a rotor diameter 400 mm x 6500 mm, weight 6000 kg, forged										
heat treatment	austenitization 1050°C 7h / oil + 570°C 10.25 h / air + 690°C 10h / air										

Table 1: Chemical composition (weight %) and heat treatment of X12CrMoWVNbN10-1-1

Experimental details

Experiments were carried on an electric-mechanical servo machine with a maximum force capacity of ±100KN (Fig. 2a). The specimen was heated with a controlled three-zone-convention-furnace, which keeps homogeneous temperature distribution advantageously. The temperature was measured by a PtRh-Pt thermocouple of type S at mid gauge section during testing. Two extra thermocouples were fixed on the both tension rods (Fig. 2b) in order to control the temperature homogeneity. The temperature variations at control thermocouple positions were held to within ±3°C. The deformation was measured by inductive distance sensor with analog output (Fig. 2b). Fig. 3 illustrates the geometry of the specimen. Extensometer rods were placed on locations indicated with A.

All tests were carried out at 600°C. The stress-controlled test cycle was based on the service-type strain cycles [1], which is a three-stage strain collective with 1 cold start, 3 warm starts and 16 hot starts (Fig. 1). The sum of hold times amounts to one hour. Nominal stress rate subject to service condition was chosen according to an equivalent strain rate of ca. 10^{-5}/s (Fig. 4).

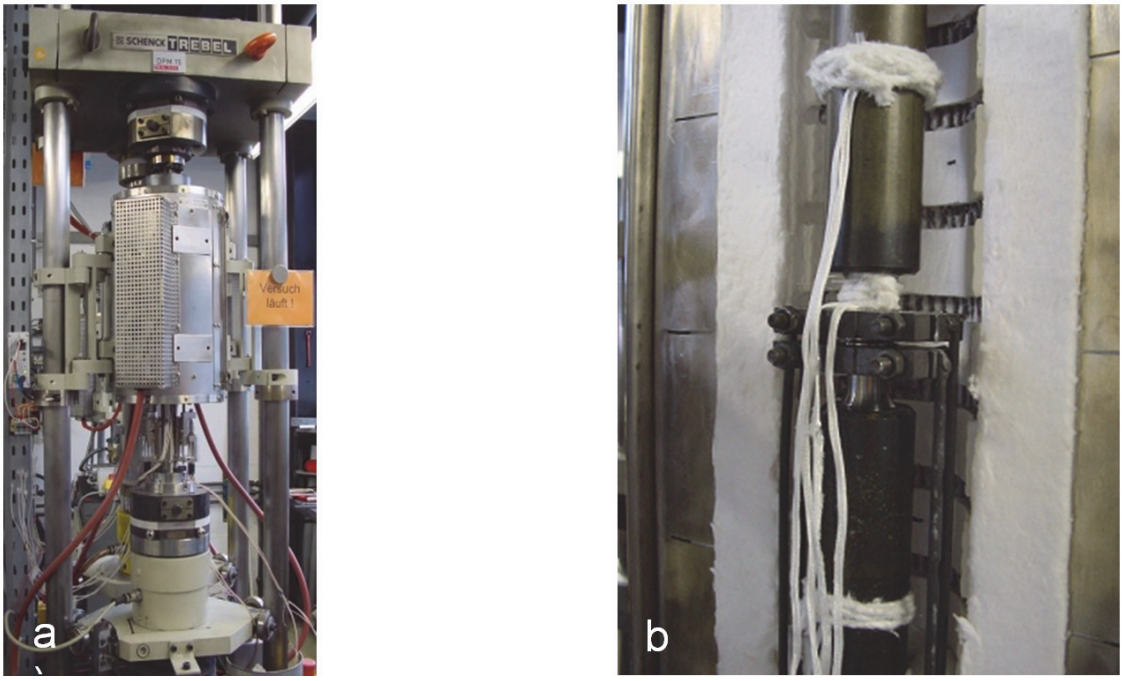

Figure 2: Equipment for testing of notched specimens, (a) electric - mechanical testing system and (b) used measurement device of the axial deformation at the edge of the notch as well as the thermocouple to measure the temperature.

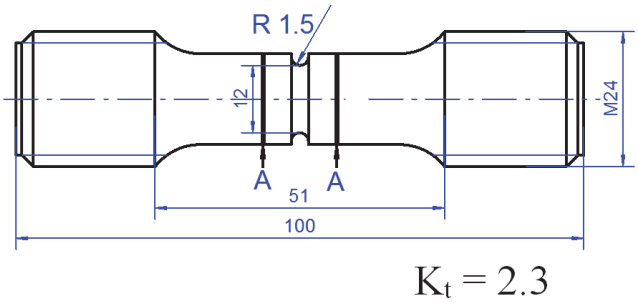

Figure 3: Specimen and dimensions of the used notched specimen (mm).

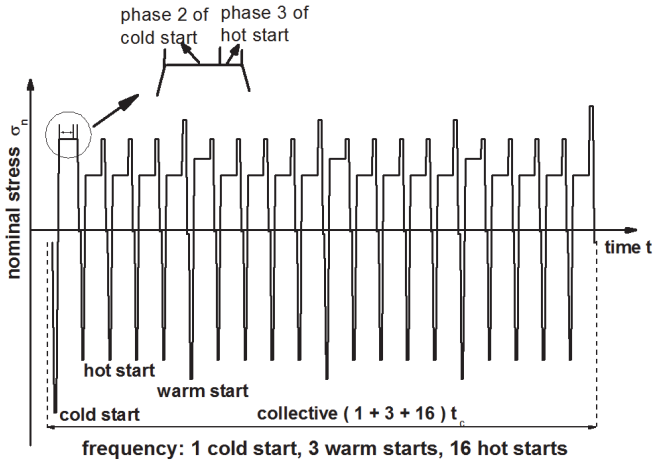

Figure 4: Force controlled loading on notched specimens with a three-stage service-type loading.

Experimental results

Tab. 2 summarizes the test results of creep-fatigue lives under the 3-stage service-type loading at temperature 600°C performed in this study, where nominal stresses are normalized in σ and in its proportion because of data protection. The stress amplitude σ/2 is just below the yield strength $R_{p,0.2\%,600°C}$ at 600°C. The total hold time $\sum t_h$ represents the summation of dwell periods within a single cycle.

The number of cycles to crack initiation N_i corresponds to crack depth $\Delta a \approx 0.5$-1mm, which is determined by analyzing the relationship between irreversible deformation energy W and the number of cycles N. Here, the procedure is introduced by example with the experiment uA16kb63 (Fig. 5). At first, Crack depth is plotted against the deformation energy W. Crack depth after tests was measured though metallographic investigations. It is assumed that the initial crack depth at the end of linear behavior of deformation energy W is zero. In Fig. 5a, it is observed that irreversible deformation energy W increases linearly up to ca. ¾ of the test duration. The deformation energy W by crack depth of 0.5mm was resulted from a linear interpolation in Fig. 5b, and with this value, the number of cycles of crack initiation Ni was determined in Fig. 5a.

test piece ID	T (°C)	$\sum t_h$ (h)	$\Delta\sigma_{n,c}$ /$\Delta\sigma_{n,w}$ /$\Delta\sigma_{n,h}$ (MPa)	N_i[a)] (-)	t_i[a)] (h)
uA16kb60	600	1	2.78σ/2.35σ/2.00σ	441	523
uA16kb61	600	1	2.36σ/2.00σ/1.70σ	801	928
uA16kb62	600	1	2.08σ/1.76σ/1.50σ	2733	3000
uA16kb63	600	1	1.39σ/1.17σ/σ	7547	8284

a) crack initiation, crack depth 0.5-1 mm

Table 2: Summary of the test results under service-type loading on notched specimens

The numbers of cycles to fracture N_f and to crack initiation N_i in relationship to nominal stress range $\Delta_{\sigma n}$ are summarized in Fig. 6, where the nominal stress range of hot start cycles $\Delta_{\sigma n,H}$ is applied to represent the 3-stage service-type cycles. The solid line was generated from uniaxial push-pull tests without dwell time [2][3]. The both dashed lines represent creep fatigue lifetime with 1h and 3h dwell time [2, [3] at maximum and minimum load on notched specimens with the same specimen type used in this paper (Fig. 3). The four life data performed in this paper are shown as filled circles in Fig. 6. Endurances to crack initiation of service-type with total dwell time of 1h are similar to life of fracture from 1h/1h push-pull test results (dashed line). The difference between life of fracture N_f and life of crack initiation N_i is estimated about 10%. In general, increasing loading period leads to a reduction of lifetime due to high influence of the creep damage during the dwell time. This is caused by the high ductility of the examined 10%Cr-steel and the high influence of the creep damage during the hold times. The four life data performed in this paper are subordinated to prior results. The lower load rate, which induces more creep damage, is also another reason to reduce lifetime.

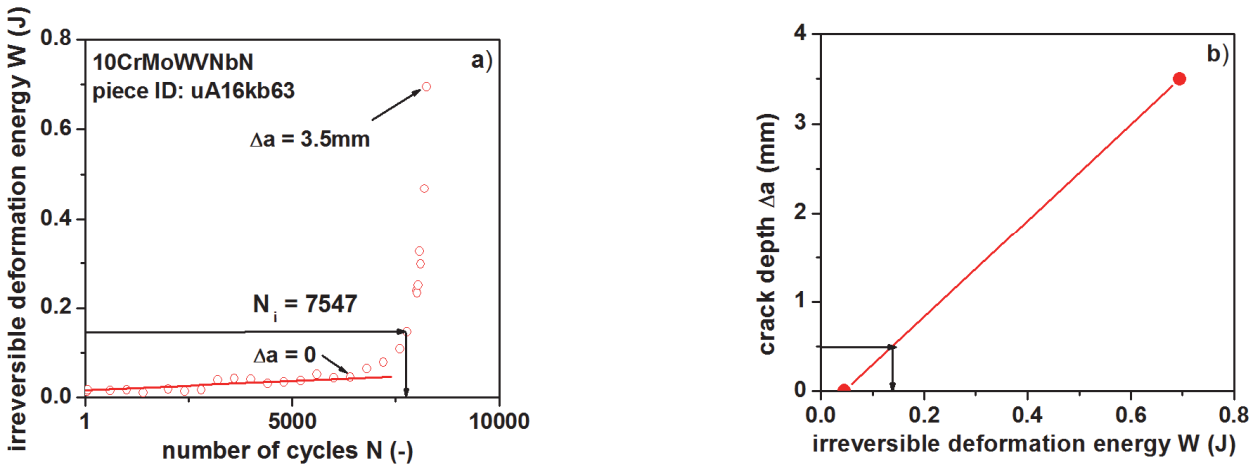

Figure 5: (a) Irreversible deformation energy W against number of cycles N and (b) crack depth Δa against irreversible deformation energy W, specimen uA16kb63.

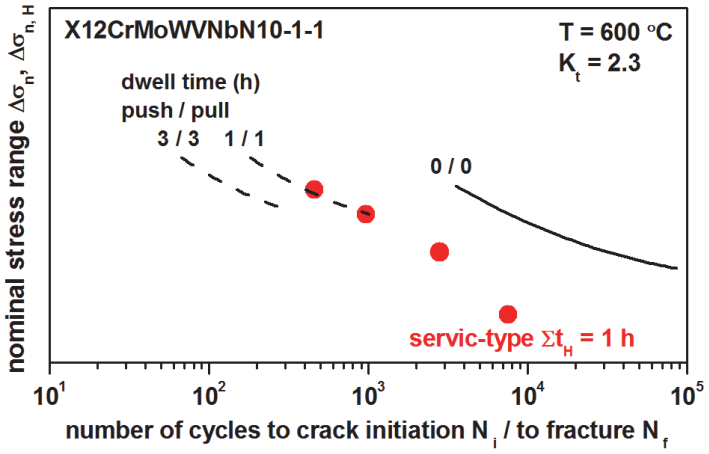

Figure 6: Characteristic lines of experiments without and with dwell time at maximum and minimum nominal stress [2][3] as well as the service-type data on notched specimens.

Fig. 7 correlates an overview of measured maximum and minimum peak-values of axial deformations as well as mean values of the 3-stage service-type experiments in relation to the number of cycles. The peak-values of axial deformation are drifting down with a constant rate at the beginning of the tests. The peak-values of specimens of uA16kb60 and uA1kb61 decrease after that quickly (Fig. 7 a, b). The both specimens were loaded under relative high nominal stress, whose amplitudes are substantially higher than yield strength $R_{p,0.2\%,600°C}$. In contrast, the axial deformation peak-values of specimens of uA16kb62 and uA16kb63 decrease after that slowly until the cycle number to about 2000 (Fig. 7 c,d). After that, the peak-values drift up against the number of cycles with an increase of deformation range, which indicate the initiation of micro cracks in microstructure.

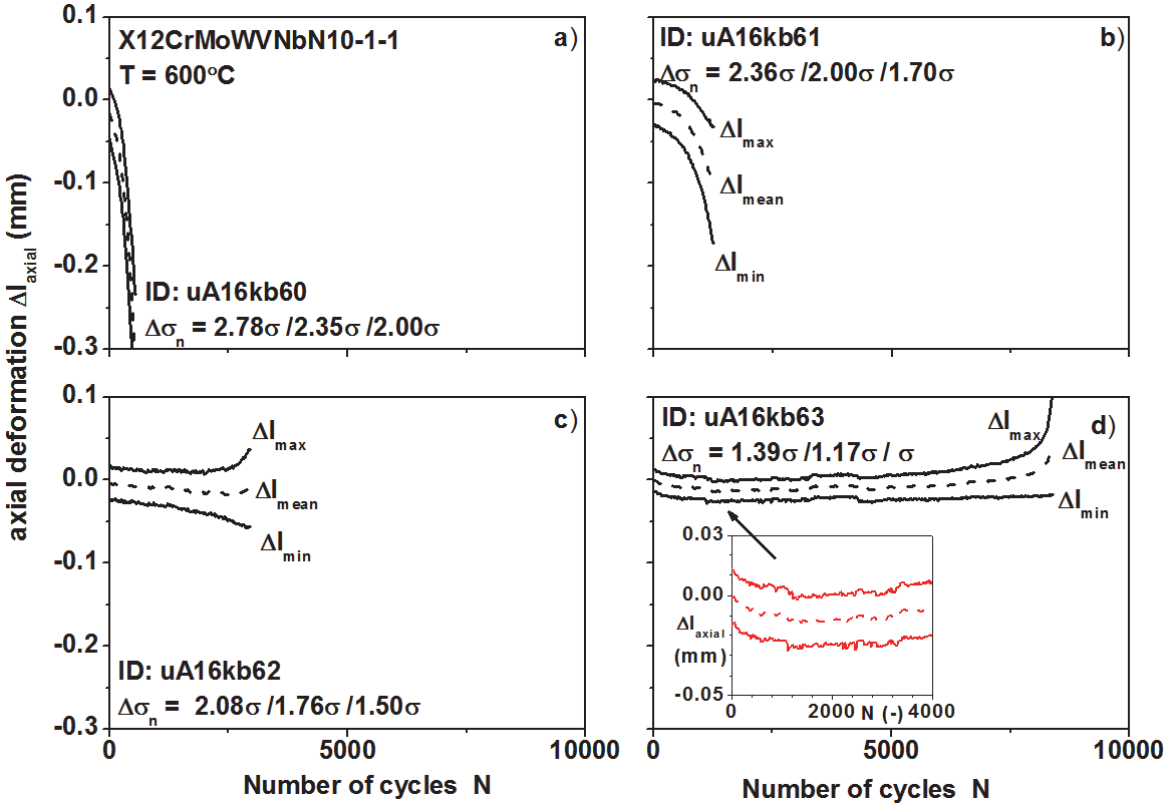

Figure 7: Measured maximal amplitude of axial deformations, minimal amplitude of axial deformations and mean deformations of service-type experiments on notched specimens against number of cycles according to Tab. 2.

METALLOGRAPHIC EXAMINATION

After tests, significant plastic deformation was observed at notch roots by macroscopic investigation (Fig. 8). The higher the stress range or the longer the dwell time is, the larger the deformation is. This leads to change the form factor K_t determined from notch geometry before testing. Thus it is difficult to estimate lifetime with Neuber-hypothesis.

Cracks on notch root specimens of uA16kb60 and uA16kb61 (Fig. 8a, b) are initiated obviously through extrusions in correspondence with the drifting of axial deformation peak-values into press (Fig. 7a,b). Typical fatigue dominant damage is shown by transgranular cracks which initiate from the surface along the notch shape (Fig. 8ato d). Main crack moves sometimes along grain boundaries during its course (Fig. 8e to h) representing intergranular cracking and a typical creep fatigue interaction. A complex damage was observed underneath the notch root surface (crack tips).

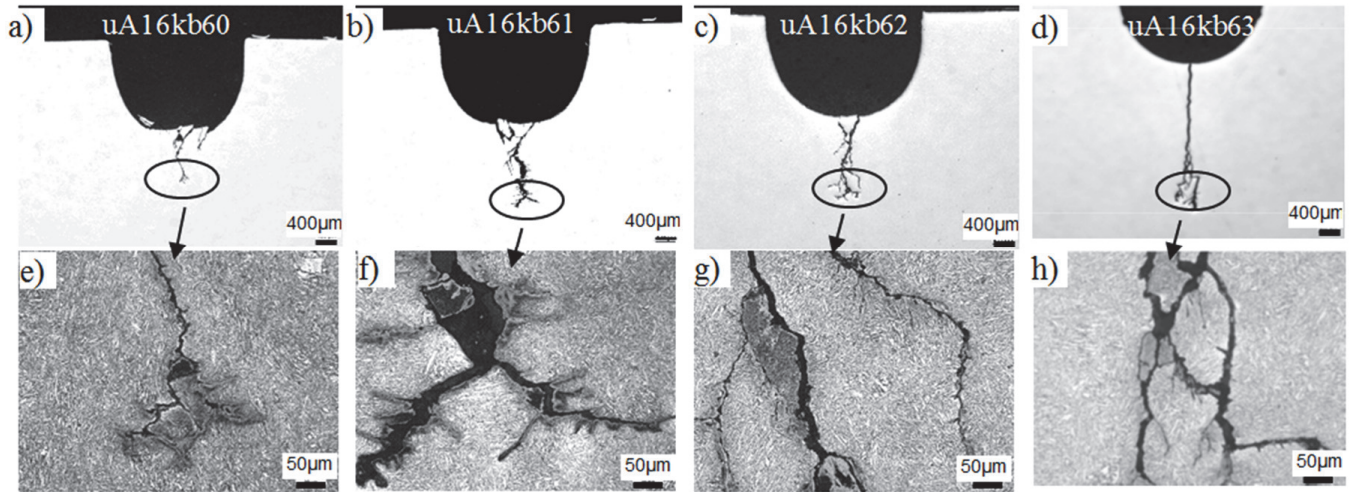

Figure 8: Crack after 3-stage service-type loading at 600°C (a) to (d) and details of the 4 marked location (e) to (h), notched specimens, X12CrMoWVNbN10-1-1.

STRESS STRAIN ANALYSES

Constitutive material model

A viscoplastic constitutive material model in accordance with Lemaitre and Chaboche with a few changes for a better adaptation to high temperature material behaviors is applied for the stress strain analysis [4, 5].

An equivalent stress f:

$$f = \sqrt{\frac{3}{2}(\mathbf{T}-\mathbf{X})^D : (\mathbf{T}-\mathbf{X})^D} \tag{1}$$

is derived from the deviator of the difference between the stress tensor T and the back stress tensor of kinematic hardening X, where the operator (...)D denotes deviator of a tensor.

The accumulated plastic strain s is used in the model, and its evolution is described as:

$$\dot{s} = \frac{\langle f \rangle^m}{\eta} \cdot e^{a \cdot f^d} \tag{2}$$

with four material parameters m, η, a and d. The power law was modified with the term $e^{a \cdot f^d}$ according to [6] for better conformance to a wide stress range.

The plastic strain flow rule is given as:

$$\dot{\mathbf{E}}_p = \frac{3}{2}\frac{(\mathbf{T}-\mathbf{X})^D}{f}\dot{s} \tag{3}$$

The evolution equation of the kinematic hardening variable Y follows the Armstrong–Frederick hardening rules with an additional static recovery term and can be written as:

$$\dot{\mathbf{X}} = c\dot{\mathbf{E}}_p - B\cdot b\mathbf{X}\dot{s} - p\mathbf{X} \tag{4}$$

where b, p and c are material parameters. A scalar function B

$$B(s) = B_1 + (1-B_1)e^{-B_2\cdot s} \tag{5}$$

represents accumulated plastic strain s; parameters B1 and B2 are applied to the dynamic recovery term describe cyclic softening behavior.
All of the above mentioned material parameters m, η, a, b, d, p, c, B1 and B2 were determined by uniaxial creep tests and push pull tests with analytical fits at 600°C. The material model was implemented in the finite element analysis program ABAQUS by means of a user subroutine UMAT, in which the differential equations of the material model are numerically integrated using the Runge-Kutta method [5].

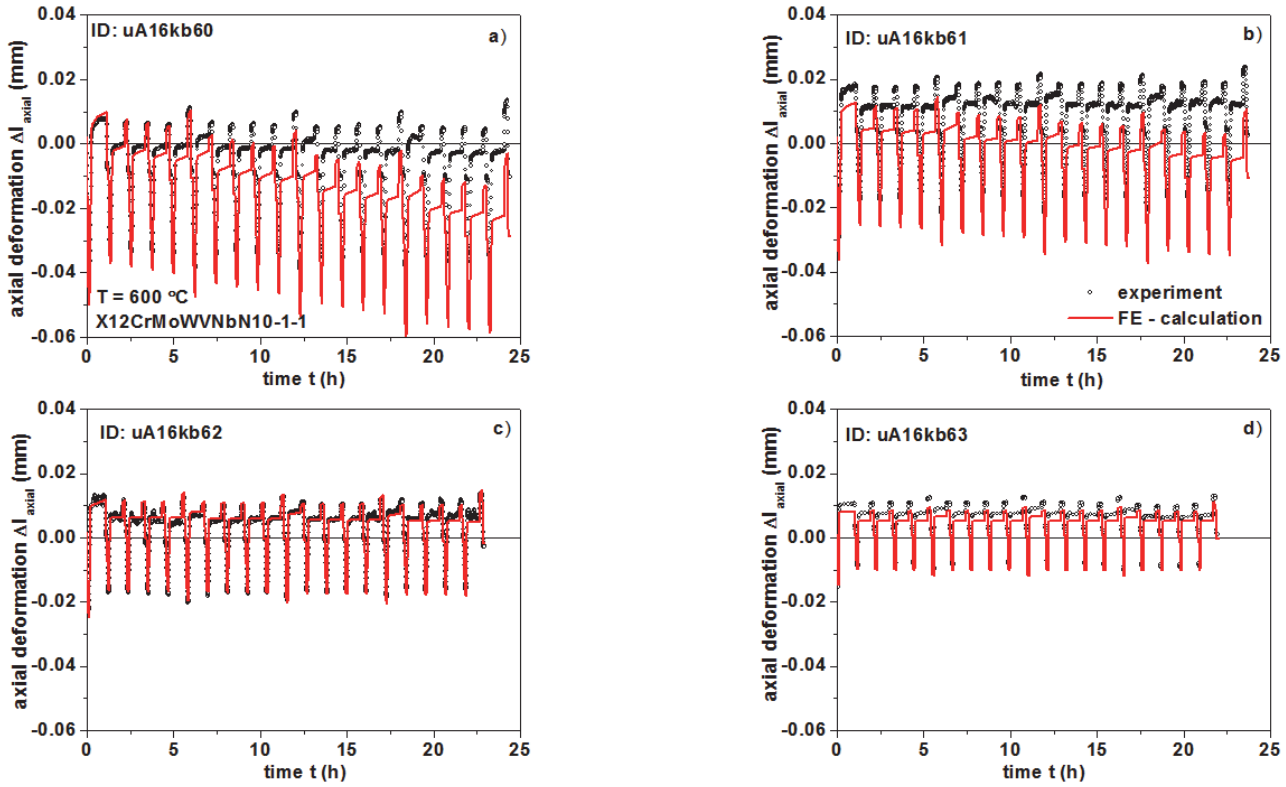

Figure 9: Comparing of axial deformation between two positions A marked in Fig.3, FE – calculation (material model from [4][6]) in comparison with experiment.

Finite-element analysis

Nonlinear finite-element calculations were performed in order to determine the stress-strain behavior at notch during 3-stage service-type loading. According to axis symmetry of the specimen shape a quarter of the specimen was modeled by a FE mesh. An axisymmetric mesh with quad elements was employed.

Plotting the axial deformation vs. testing time, the simulation provides an acceptable agreement with experimental values for the first 20 sub-cycles in all 4 tests (Fig. 9). In tests with larger stress amplitudes, which means that the maximum nominal stress is bigger than 0.2% yield strength at the testing temperature, the displacement drifts into compression domain with an increasing number of cycles (Fig. 9a, b). The ratcheting effect is overestimated by the material model for the tests uA16kb60 and uA16kb61. The influence of material damage on the deformation was considered in the FEA. However, the impact of damage in the first cycle of sequence plays no significant role, therefore it is not the reason for overestimating ratcheting. In contrast, the simulation describes the deformation of the experiments with lower nominal stress (uA16kb62 and uA16kb63) pretty well (Fig. 9c, d). The maximum of the equivalent loading is located at the notch root in accordance with the FEA, thus the simulation results at the corresponding node is applied for lifetime prediction.

LIFETIME ESTIMATION

A phenomenological lifetime estimation approach developed for service-type loading (Fig.1) was based on rules for synthesis of stress strain path, wherein mean stress effect and creep fatigue interaction are include. For life estimation under service-type creep fatigue loading, the life fraction rule proposed by Robinson/Taira [7] was implemented in the approach. Crack initiation is determined by the summation of fatigue damage D_f representing a cyclic fraction and creep damage D_c representing a time fraction summing up to the number of cycles to crack initiation N_i:

$$D_c + D_f = \sum_{1}^{N_j}\left(\sum_{1}^{k}\sum_{1}^{n}\frac{\Delta t_{k,n}}{t_{u,k,n}} + \frac{1}{N_{io,j}}\right) = D \tag{6}$$

The creep damage for one hold phase is calculated as the accumulation of the ratio of time increments $\Delta t_{k,n}$ to rupture time $t_{u,k,n}$ during the hold phase. The rupture time $t_{u,k,n}$ is carried out according to the instantaneous acting load and temperature from rupture characteristic curves, which were generated by data of static creep tests. The fatigue damage D_f is calculated by a reference number of cycles to crack initiation N_{io}, which is determined under consideration of creep fatigue interaction and mean stress effect. The creep fatigue interaction was developed in a previous paper according to metallographic damage [8]. The material-specific mean creep fatigue damage of 0.68 for the material X12CrMoWVNbN10-1-1 determined by uniaxial service-type tests [8] was used as a critical damage value D_{crit} in this paper.

Phenomenological life time calculation requires scalar stress and strain values. Hence the maximum principal stress σ_1 and the von Mises equivalent stress σ_V were calculated for one point at the surface of the notch root with the help of the constitutive material model introduced above. The maximum principal stress σ_1 is equal to the stress in axial direction σ_{22}. The hysteresis loop σ_{22} (ε_{22}) represents a corresponding uniaxal loading.

In Fig. 9 the signed equivalent stress $\sigma_{V,1}$ gets its sign form the maximum principal stress σ_1:

$$\sigma_{V,1} = \sigma_V \cdot sign(\sigma_1) \text{ with } \sigma_V = \sqrt{\frac{3}{2}\mathbf{T}^D \cdot \mathbf{T}^D} \text{ and } \sigma_1 = \sigma_{22} \tag{7}$$

The directions of the elastic equivalent strain ε_{Ve} and the plastic equivalent strain ε_{Vp} are also associated with the sign of the maximum principal stress σ_1:

$$\varepsilon_{V,1} = \varepsilon_{Ve,1} + \varepsilon_{Vp,1} = \frac{\sigma_{V,1}}{E} + \int_0^t \dot{s} \cdot sign(\sigma_1)\, dt \tag{8}$$

The equivalent strain range Δ_{eV} is used for estimation of the fatigue damage with the uniaxial low cycle fatigue curve representing a hold time of t_H = 1h. The equivalent stress is used for estimation of the creep damage.

For stress-controlled loading the mean stress is constant and the mean strain varies during testing. As Fig. 10 observed, a significant drifting of the mean axial deformation is observed. Therefore, the Smith-Waston-Topper parameter P_{swt} [8] is modified as follows:

$$P_{SWT,\varepsilon} = \sqrt{\left(\frac{\Delta\varepsilon}{2} + \varepsilon_m\right) \cdot E \cdot \frac{\Delta\sigma}{2}} \tag{9}$$

with $\Delta\sigma$ as constant stress range and ε_m as mean strain.
As an alternative to the approach described above, the Neuber-hypothesis can be used to determinate the maximum stress and strain by using cyclic tensile curves. However the hypothesis is not applicable on the experiments uA16kb60 and uA1kb61, because the high nominal stress leads to significant plastic deformation. By simulating the experiments with the material model, the mean strain cannot be described satisfactorily, which leads to a very conservative lifetime estimation (Fig.10). Thus, the mean strain is read from measured value at half-life cycle to represent the "saturated" material state.
By considering the mean strain effect, the lifetime can be predicted within a scatter band of factor 2 (Fig. 10).
To summarize, lifetime estimation without considering mean strain is conservative. The Neuber hypothesis has its strength in its easy applicability. But its application is limited to the elastic domain and it leads to strong conservatism in lifetime estimation. The application of equivalent stress and equivalent strain determined with FE analysis based on the material model of type Chaboche [6] appears relatively expensive in terms of parameter identification from current level of technology. However, it has more potential on describing complex loading because it can better represent the deformation under the complex loading.

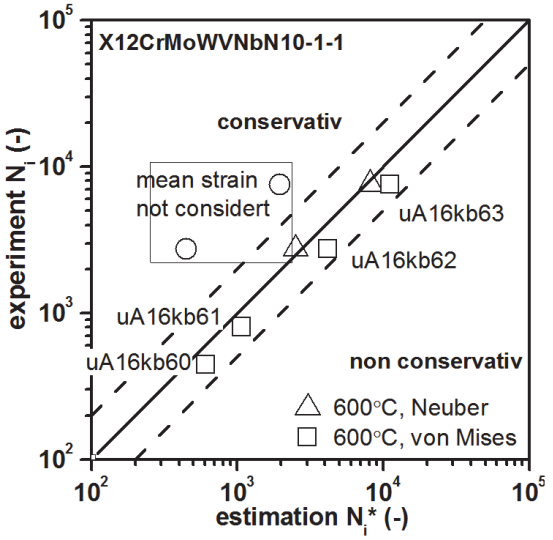

Figure 10: Correlation between estimated life N^*_i and measured life N_i.

CONCLUDING REMARKS

Service-type experiments were carried out on notched specimens of the X12CrMoWVNbN10-1-1 rotor steel under cyclic creep fatigue loading at service temperature 600°C. The peak-values of deformation decrease quickly if the loaded nominal stress is higher than the material's 0.2% yield strength at the testing temperature. At lower nominal stress, the peak-values decrease slowly and almost linearly until about 2000 cycles and then they increase again.
According to metallographic investigations on the 4 tested specimens, cracks are perpendicular to the direction of loading and propagate from the surface of the notch root. Crack initiations are transgranular and clearly through extrusions on the surface. The main transgranular cracks ramified during its propagation.
The lifetime of the 4 test specimens was estimated with a phenomenological lifetime prediction method by using Neuber hypothesis and equivalent stress/strain in the gauge part of the specimens. The uniaxial equivalent stress was determined with von Mises from finite-element-analysis according to constitutive material model of type Chaboche.
The estimated life and experiment are predicted in a scatter band of factor 2, while the results are conservative by using Neuber hypothesis if the effect of mean strain on lifetime estimation is not considered.

ACKNOWLEDGEMENT

Thanks are due to the Forschungsvereinigung der Arbeitsgemeinschaft der Eisen und Metall verarbeitenden Industrie e.V. (AVIF-No. A232) and National Natural Science Foundation of China (No. 51305348) for financial support.

REFERENCES

[1] Samir, A., Simon A., Scholz A., Berger C., Service-type creep-fatigue experiments with cruciform specimens and modelling of deformation, International Journal of Fatigue, 28(5-6) (2006) 643-651.
[2] Schwienheer, M., Scholz, A., Haase, H., Berger, C., Influences of hold times and notches on life time under service-type creep fatigue loading, Proceedings of Fifth International Conference on Low Cycle Fatigue, LCF 5, Berlin, DVM, (2003) 245-250.
[3] Schwienheer, M., Hochtemperaturverhalten der 600°C-Dampftubinenstähle (G)X12CrMoWV-NbN10-1-1, Dissertation TU-Darmstadt, D17 (2004).
[4] Simon, A., Scholz A., Berger C., Validation of creep fatigue lifetime calculation methods for the application to steam turbine rotors, Variable Amplitude Loading, Darmstadt, Proceedings, DVM, I (2009), 505-516.
[5] Tsakmakis, C., Reckwerth, D., The Principle of Generalized Energy Equivalence in Continuum Damage Mechanics, Deformation and Failure in Metallic Materials, Springer Verlag (2003).
[6] Wang, P., Cui, L., Scholz, A., Linn, S., Multiaxial thermomechanical creep-fatigue analysis of heat-resistant steels with varying chromium contents, International Journal of Fatigue, 67(2014) 220-227.
[7] Taira, S., lifetime of structures subjected to varying load and temperature, in Creep in structure, J. ed. Academic press, New York (1960) S. 96/124.
[8] Scholz, A., Berger, C, Deformation and life assessment of high temperature materials under creep fatigue loading, Mat.-wiss. u. Werkstofftechn. 36(11) (2005) 722 – 730.